Materials Science and Engineering C 48 (2015) 71–79

Contents lists available at ScienceDirect

Materials Science and Engineering C

journal homepage: www.elsevier.com/locate/msec

Development of nanofibrous scaffolds containing gum tragacanth/poly (ε-caprolactone) for application as skin scaffolds

Marziyeh Ranjbar-Mohammadi [a], S. Hajir Bahrami [a,b,*]

[a] Textile Engineering Department, Amirkabir University of Technology, Tehran, Iran
[b] Center for excellence Modern Textile Characterization, Tehran, Iran

ARTICLE INFO

Article history:
Received 14 May 2014
Received in revised form 22 August 2014
Accepted 8 October 2014
Available online 13 October 2014

Keywords:
Electrospinning
Nanofiber
Cell culture
Gum tragacanth
Poly (ε-caprolactone)

ABSTRACT

Outstanding wound healing activity of gum tragacanth (GT) and higher mechanical strength of poly (ε-caprolactone) (PCL) may produce an excellent nanofibrous patch for either skin tissue engineering or wound dressing application. PCL/GT scaffold containing different concentrations of PCL with different blend ratios of GT/PCL was produced using 90% acetic acid as solvent. The results demonstrated that the PCL/GT (3:1.5) with PCL concentration of 20% (w/v) produced nanofibers with proper morphology. Scanning electron microscopy (SEM) and differential scanning calorimetry (DSC) were utilized to characterize the nanofibers. Surface wettability, functional groups analysis, porosity and tensile properties of nanofibers were evaluated. Morphological characterization showed that the addition of GT to PCL solution results in decreasing the average diameter of the PCL/GT nanofibers. However, the hydrophilicity increased in the PCL/GT nanofibers. Slight increase in melting peaks was observed due to the blending of PCL with GT nanofibers. PCL/GT nanofibers were used for in vitro cell culture of human fibroblast cell lines AGO and NIH 3T3 fibroblast cells. MTT assay and SEM results showed that the biocomposite PCL/GT mats enhanced the fibroblast adhesion and proliferation compared to PCL scaffolds. The antibacterial activity of PCL/GT and GT nanofibers against *Staphylococcus aureus* and *Pseudomonas aeruginosa* was also examined.

1. Introduction

Skin is the first line of physical barrier from the external factors. Its form and function can be degenerated due to several reasons such as burns, accidents, and diseases, and recovery to its original form can take several weeks or months [1]. Depending on the healing ability and type of wounds, suitable skin substitute system should be applied for providing an extracellular matrix for the natural infiltration of surrounding cells [2]. An ideal skin substitute should provide an optimal healing property with sufficient exudate absorbability, oxygen permeability and controlled fluid loss in which healing and cosmetic appearance of the injured part can occur at a maximum rate [3].

Nanofibrous scaffolds due to their pore-size distribution, high surface-to-volume ratio and most importantly, morphological similarity to natural extracellular matrix (ECM) may be used as wound dressing scaffolds [4–6]. Among the different ways of nanofiber production, electrospinning appears to be a simple, superior, smart and scalable technique to fabricate polymeric nanofibers [7]. Natural and synthetic polymers cannot provide all the requirements of a perfect nanofibrous scaffold exclusively for application as wound dressing or skin scaffold. Natural polymers lose their mechanical properties very quickly during degradation while synthetic polymers, such as polyesters are usually hydrophobic, have less binding sites for cell adhesion and release acidic products during degradation. To overcome the aforesaid problems and provide desirable new biomaterials, hybrid materials which are blends of two or more types of polymers have been fabricated by researchers that assimilate the desirable characteristics of component materials [8].

Gum tragacanth (GT), a natural polymer, is known for its excellent biological properties such as biodegradability, biocompatibility, antibacterial and wound healing activity [9]. This hydrocolloid has been accepted since 1961 as GRAS at the level of 0.2–1.3% and in Europe has E-number E413 on the list of additives approved by the Scientific Committee for Food of the European Community [10]. Mucilage of GT is used in lotions for external applications and, at higher concentrations, as a base for jelly lubricants and in medicinal oil emulsions. As an emulsifier, it facilitates the absorption of poorly soluble substances such as steroid glycosides and fat-soluble vitamins. This gum is also used in various types of elixirs and syrups where low-calorie intake is required [9,11]. In our previous work, GT was blended with poly(vinyl alcohol) to improve the spinnability of GT solution, then nanofibers were chemically cross-linked with glutaraldehyde. The smooth surface nanofiber showed good antimicrobial property against gram-negative bacteria (*Pseudomonas aeruginosa*), however human fibroblast cells had well attachment and proliferation on these scaffolds [12]. There is no available report on the production of electrospun GT composite scaffolds with PCL, PLGA, etc.,

* Corresponding author.
E-mail address: hajirb@aut.ac.ir (S.H. Bahrami).

http://dx.doi.org/10.1016/j.msec.2014.10.020
0928-4931/

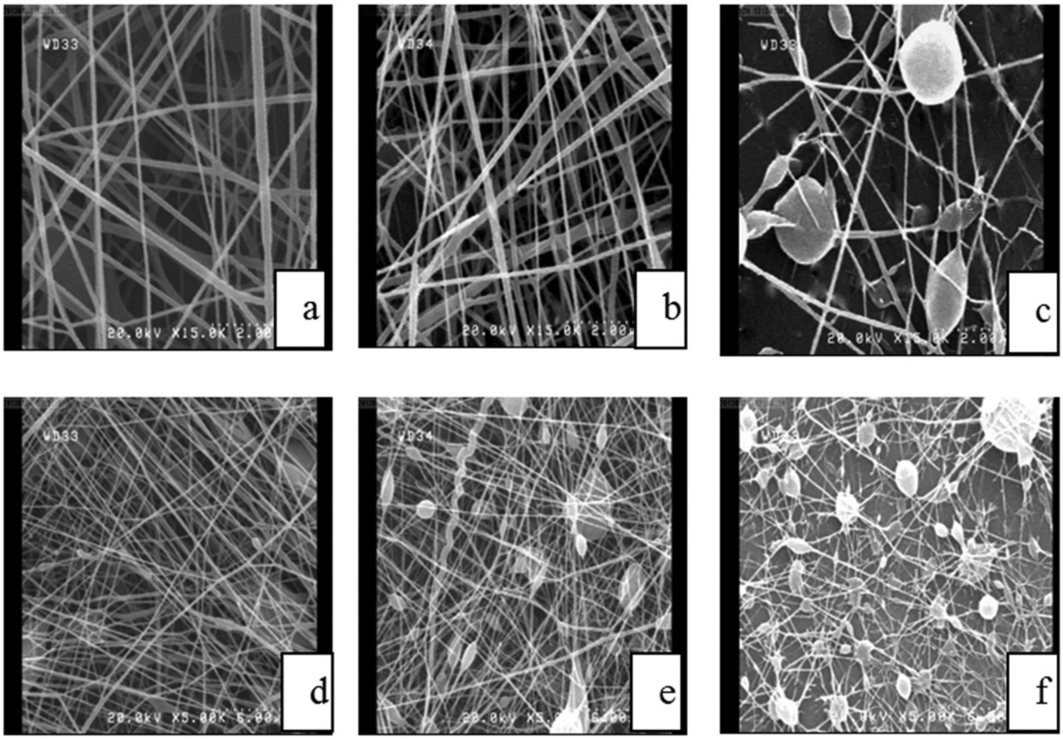

Fig. 1. SEM micrographs of PCL (10 w/v %)–GT (7 w/v %) blend nanofibers with different blend ratios: a, d) 3:0, b, e) 3:1, and c, f) 3:1.5 electrospun under applied voltage 15 kV, extrusion rate 0.5 mL/h and nozzle to collector distance 20 cm; (a, b, c) 15,000×, (d, e, f) 5000×.

and their applications in either skin tissue engineering or wound healing. Poly (ε-caprolactone) (PCL) is an aliphatic polyester, often used in biomedical applications because of its biocompatibility, slow biodegradability, low-cost, non-toxicity and good mechanical properties. However, it is hydrophobic [13] which may severely limits its use in certain applications. The aim of this work is to fabricate composite scaffolds from PCL and the natural biopolymer GT at varying ratios. Further we investigated the mechanical properties, hydrophilicity, biocompatibility and fibroblast cell proliferation of nanofibers for wound dressing application.

2. Materials and methods

2.1. Materials

Gum tragacanth used in this study was a high quality ribbon type, collected from the stems of floccosus species of Astragalus bushes, growing in central areas of Iran. The raw gum was ground into fine powder. The moisture content of the gum powder was measured using the standard method of AOAC [14]. The density of GT was measured by

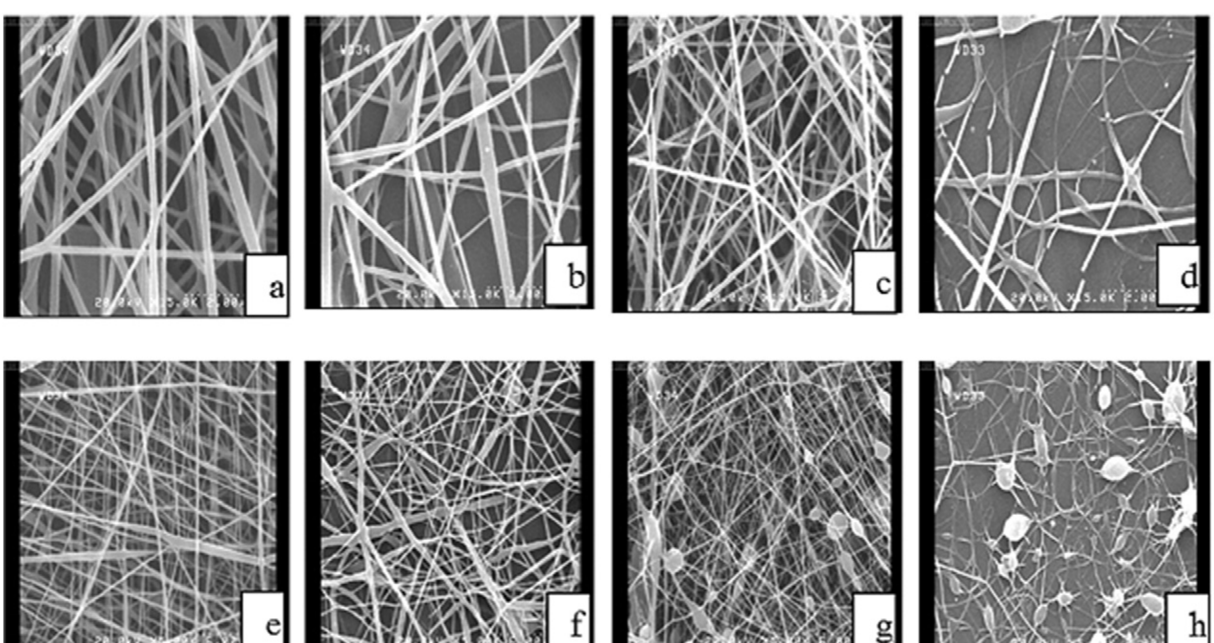

Fig. 2. SEM micrographs of PCL (15 w/v %)–GT (7 w/v %) blend nanofibers with different blend ratios: a, e) 3:0, b, f) 3:1, c, g) 3:1.5, and d, h) 3:3 electrospun under applied voltage 15 kV, extrusion rate 0.5 mL/h and nozzle to collector distance 20 cm); (e, f, g, h) 5000×, (a, b, c, d) 15,000×.

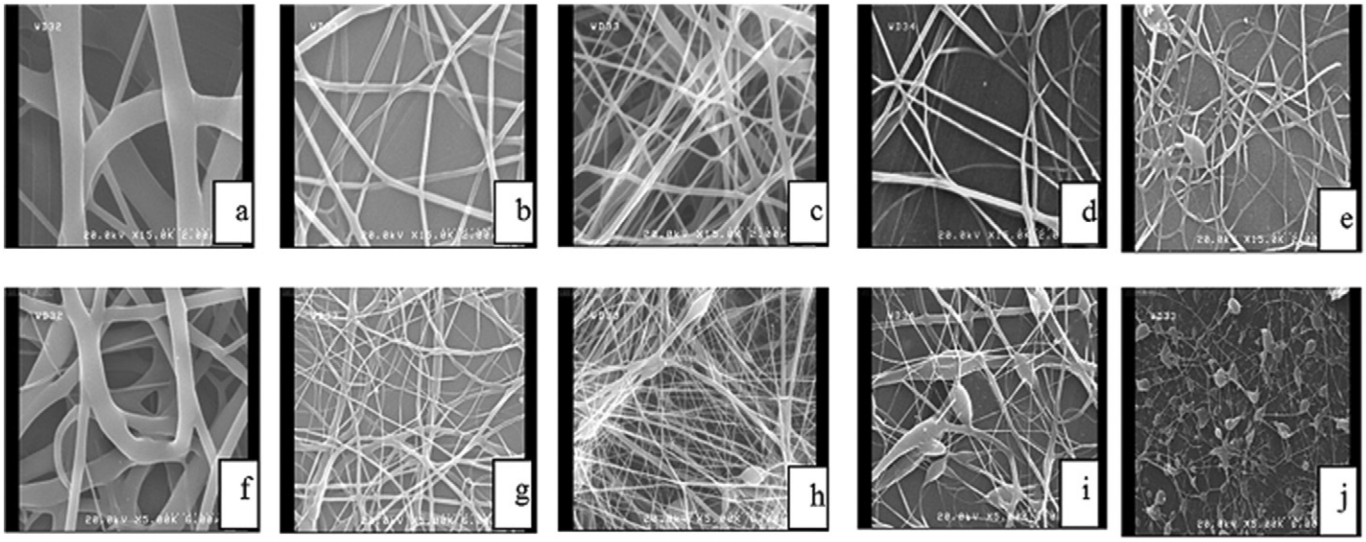

Fig. 3. SEM micrographs of PCL (20 w/v %)–GT (7 w/v %) blend nanofibers with different blend ratio: a, f) 3:0, b, g) 3:1, c, h) 3:1.5, d, i) 3:3, and e, j) 3:6 electrospun under applied voltage 15 kV, extrusion rate 0.5 mL/h and nozzle to collector distance 20 cm; 5000×, 15,000×.

Table 1
Viscosity (mPa/s) of PCL and PCL/GT (3:1.5) at room temperature.

PCL (10 w/v %)	PCL (15 w/v %)	PCL (20 w/v %)	PCL (10 w/v %)/GT	PCL (15 w/v %)/GT	PCL (20 w/v %)/GT
700	1800	2400	300	800	1400

using a pycnometer with ethanol as the media. The density and moisture content of GT were 1.42 g/cm^3 and 11.4 wt.% respectively. PCL (Mw 80 kDa) was purchased from Sigma-Aldrich; Glacial acetic acid was purchased from Merck Co. All the materials were used without any purification. 7% solutions of GT in 90% acetic acid were mixed with different concentrations of PCL (10, 15, 20% (w/v)). PCL was dissolved in 90% acetic acid (90% AA). Other chemicals were of laboratory grades and were used without any purification.

2.2. Electrospinning apparatus

The electrospinning apparatus used in this work consisted of a high voltage power supply, a syringe pump, a stainless steel spindle and an aluminum plate-type collector. To produce nanofibers, the syringe was filled up with the polymeric solution and a high voltage was applied to overcome the surface tension of the polymer solution, and then a charged jet is ejected. The jet extends in a straight line for a certain distance and then bends and follows a looping and spiraling path. These jets were collected on an aluminum foil as nanofibers. All electrospinning were carried out at room temperature. Electrospinning was carried out with constant feeding rate, tip-target distance and applied voltage of 1 mL/h, 15 cm and 15 kV, respectively.

2.3. Characterization

The morphology and diameters of nanofibers were studied with the use of FESEM (XL30-SFEG, 12 FEI/Phillips, and Japan) at an accelerating voltage of 20 kV. For SEM, the samples were coated with gold using sputter-coater operated at 15 kV for 80 s. The average diameter of the nanofibers was measured and calculated from 100 random points chosen from the SEM images, using image analysis software (Image J, National Institute of Health, Bethesda, MD). Fourier transform infrared spectroscopy (FTIR) analysis (Nicolet Magna-IR 560) was used to study the structural changes using KBr method for GT powder and PCL, PCL/GT nanofibers. Thermal properties were examined by differential scanning calorimetry (Mettler Toledo, Switzerland) and samples were heated from −110 °C to 310 °C at a heating rate of 10 °C/min under nitrogen. The viscosity of the polymer solutions was measured using a Brookfield viscometer (Model DV-II + Pro).

The tensile behavior of the electrospun nanofibers was examined on an Instron (model 5566 made in UK) using a 10-N load cell under a cross-head speed of 10 mm/min at room temperature. All nanofiber tape samples were prepared in the form of rectangular shape with dimensions of 30 × 10 mm^2. Mechanical characterization was performed by applying test loads to specimens prepared from the electrospun nanofibers. At first, a white windows paper template was cut and nanofibrous tapes were glued onto the top and bottom areas of window. It was placed between the grips of the tensile testing machine and after closing the grips, the other sides of the window papers were cut by scissor. The reported results are the average of five specimens [15].

To study the degradation behavior of the scaffolds, the fibers on aluminum foil were placed in a 12-well plate containing 1 mL of phosphate buffer solution (PBS; pH 7.4) and incubated at 37 °C for 30 days. The fresh media were added after every 3 days. After the degradation period, the samples were dried and FESEM images were taken.

The solutions of PCL 20%, PCL/GT (3:1.5) and GT in 90% acetic acid solution were prepared. Surface tension measurements of 5 mL from each solution were carried out using a Du Nouy ring tensiometer (Krüsstensiometer K 100SF). All measurements were made at 20 °C. The experiments repeated three times for each sample.

The apparent density of scaffolds was calculated from Eq. (1) in which the porosity of scaffolds was determined from Eq. (2) [16]. The apparent web density of PCL and PCL/GT blend nanofibers was estimated according to average density from Eq. (3). The density (g/cm^3) of the

Table 2
Surface tension of polymer solutions for electrospinning.

Polymer solution in acetic acid solution	γ (mN/m)
GT (7 w/v %)	38
PCL (20 w/v %)	31
PCL/GT (3:1.5)	29

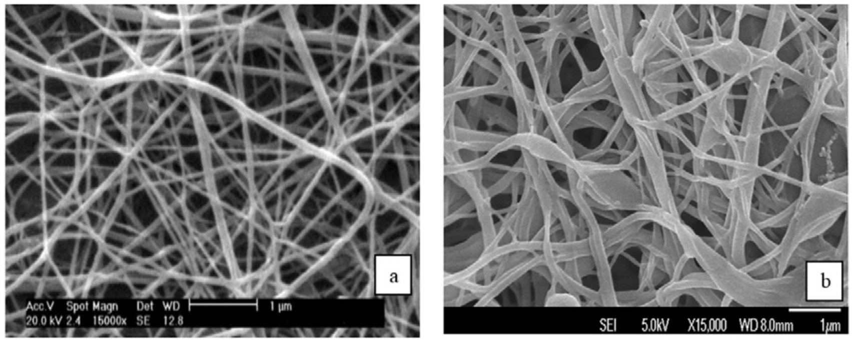

Fig. 4. SEM images of a) electrospun PCL/GT nanofibers before degradation, b) PCL/GT nanofibers after 30 day degradation.

PCL/GT blend solid film (manufactured by a solution casting method) and the thickness of the nanofiber mats was measured by a micrometer. The density of PCL and GT which were used in this work was 1.14 g/cm^3 and 1/42 g/cm^3 respectively.

$$\text{Apparent density of scaffold}\left(\text{g/cm}^3\right) = \frac{\text{mass of scaffold (g)}}{\text{Area of scaffold}\left(\text{cm}^2\right)\times\text{Thickness of scaffold (cm)}} \tag{1}$$

$$\text{Porosity of scaffold} = 1 - \frac{\text{Appranet density of scaffold}\left(\text{g/cm}^3\right)}{\text{Bulk density of the material}\left(\text{g/cm}^3\right)} \tag{2}$$

$$\frac{1}{\rho_{tot}} = \frac{\text{wt\%}_{PCL}}{\rho_{PCL}} + \frac{\text{wt\%}_{GT}}{\rho_{GT}} \tag{3}$$

In order to determine the hydrophilic/hydrophobic properties of the PCL and PCL/GT nanofibers, the contact angle of nanofibers was measured by the sessile drop method for which a video contact angle instrument (KRÜSS G10, Germany) was used. The experiments were carried out at room temperature. First the electrospun mats were cut into a rectangular shape (20 mm × 20 mm) and fixed into the custom made sample holder of the drop shape analyzer and then about 1 μL of distilled water was pipetted onto the mats and temporal images of the droplet were taken using a camera and the contact angles were measured by the sessile drop approximation of the inbuilt software of the instrument.

2.4. Cell culture

Sterilizing of nanofibrous webs was done using UV-ray and then washing with sterilized PBS for three times. In order to facilitate protein absorption and cell attachment on the nanofiber surface, the scaffolds were soaked in a culture medium for 12 h. NIH 3 T3 and human fibroblast cells were cultured in Dulbecco's Modified Eagle Medium (DMEM) supplemented by 10% fetal bovine serum (FBS), 1% antibiotic solution at 37 °C under a humidified atmosphere of 5% CO_2, 99% relative humidity (RH). After counting cells, about 3×10^5 cells/cm^2 fibroblast cells were seeded on PCL and PCL/GT nanofibers on 24 well plates and incubated at 37 °C for cell growth. Light microscope was used to investigate cell adhesion and cell morphology after one day. The cell-seeded nanofibers were refilled with fresh medium every day. After 48 h of the experiment, the scaffolds were rinsed twice with phosphate buffer saline (PBS) and subsequently fixed in 2.5% glutaraldehyde for 2 h. The sample was then rinsed thrice with PBS for 12 h. They were immersed in osmium tetroxide 0.1% for 30 min and dehydrated in increasing concentrations of acetone (20, 30, 50, 70, 90 and 100%) for 10 min each. Finally, the samples were freeze-dried and sputter coated with gold for cell morphology observation by FESEM.

2.5. MTT assay

Cell viability and cell proliferation on PCL/GT and PCL nanofiber scaffolds were determined by using the colorimetric 3-(4, 5-dimethylthiazol-2-yl)-2, 5-diphenyltetrazolium bromide assay (MTT). Fresh culture medium was used as control. In this assay, the metabolically active cells are known to react with tetrazolium salt in MTT reagent to produce a soluble formazan dye and absorbance was measured at 570 nm using spectrophotometer. Direct and indirect cytotoxicity evaluations were used for doing this test. For direct evaluation, human fibroblast cells were plated in 90 μL of Dulbecco's modified Eagle's medium (DMEM), supplemented with 10% FBS, at a density of 10,000 cells/cm^2. After 3 days of cell seeding in 24-well dish, the original medium was removed and 1 mL fresh medium and 100 μL MTT solution were

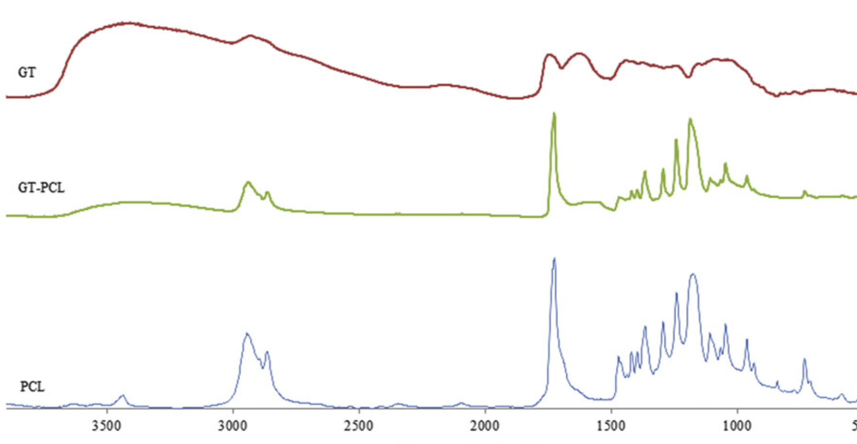

Fig. 5. FTIR spectra of samples; a) PCL, b) GT powder, and c) blend PCL/GT nanofibers.

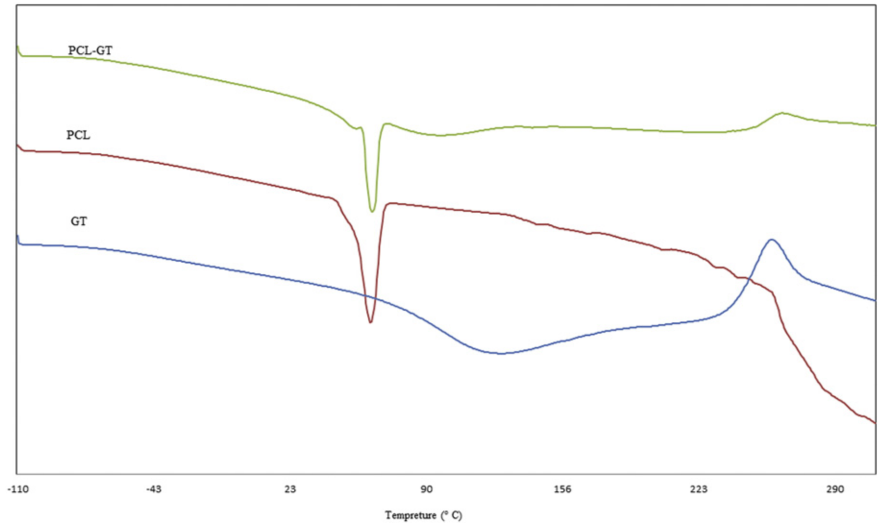

Fig. 6. DSC curves of samples; A) PCL nanofibers, B) GT powder, and C) PCL/GT nanofiber.

added to each well. Cells were allowed to incubate in the dark at 37 °C (5% CO_2) for 4 h, the medium was removed, the scaffolds were gently aspirated, and the formazan reaction products were dissolved in dimethyl sulfoxide. After 20 min of shaking, the solution was used for spectrophotometric analysis. The optical density of the formazan solution was read on a BioTekELISA plate reader at 570 nm. Indirect evaluation was done based on a procedure adapted from the ISO10993-5 standard test method [17]. The nanofiber mats of PCL/GT and PCL were immersed in a medium as described in an incubator for 24 h to produce extraction media of varying concentrations (5, 10 and 20 mg/mL). NIH 3T3 fibroblasts were seeded (1×10^4 cells/cm^2) in 96-well plate with various extracts at 37 °C under 5% CO_2/95% air condition. Cell viability was monitored at 3 days by MTT assays.

2.6. Antimicrobial properties

The antimicrobial behavior of PCL and PCL/GT nanofibers was studied by agar plate method and *Staphylococcus aureus* ATCC 25923 and *P. aeruginosa* ATCC 27853 were used as gram-positive and gram-negative bacteria respectively. Mueller-Hinton agar media was prepared and sterilized in an autoclave at 121 °C for 20 min under 15 lbs/in^2 pressure. A loop of each bacterium was inoculated on 5 mL of nutrient broth and incubated at 37 °C for 24 h, then cultured in nutrient agar plate. The disk shape samples of nanofibrous mat were sterilized by ultraviolet light for 2 h and were placed in each plate. Then the plates were held in incubator for 48 h. Photographs from samples were used for assessing the antimicrobial behavior.

2.7. Statistical analysis

All data presented are expressed as mean standard deviation (SD). Statistical analysis was carried out using single-factor analysis of variance (ANOVA). A value of $p \leq 0.05$ was considered statistically significant.

3. Results and discussion

3.1. Effect of PCL concentration and blend ratio on nanofiber morphology

The SEM images of all different compositions of PCL/GT are shown in Fig. 1. GT concentration was fixed at 7% (w/v) and PCL concentration was varied from 10 to 20% (w/v). PCL with 10% concentration was

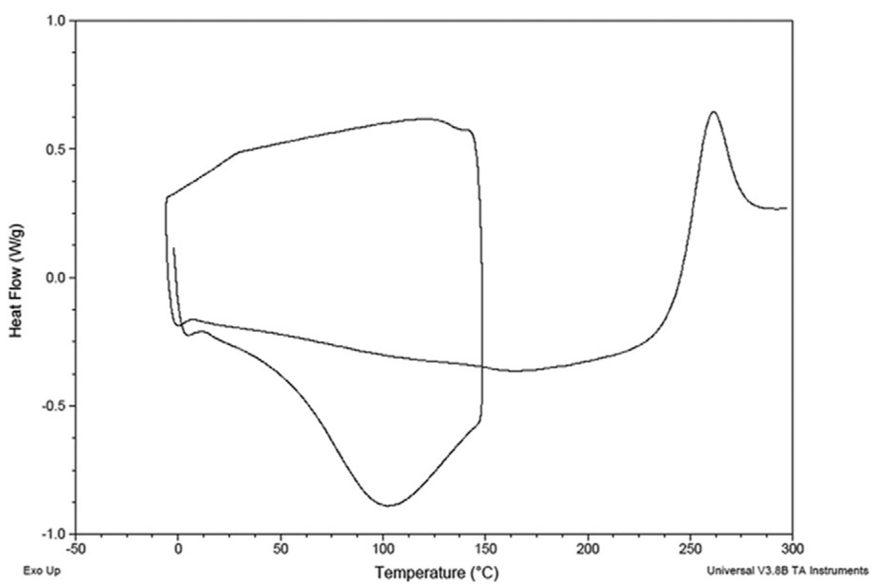

Fig. 7. Heating–cooling curve of GT powder.

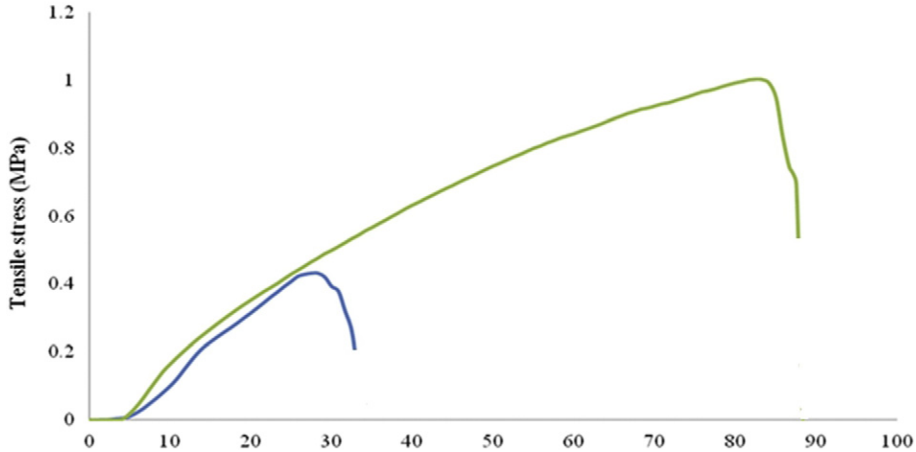

Fig. 8. Typical stress–strain curves of PCL, PCL/GT (3:1.5) nanofibers.

taken and three solutions with different compositions of PCL/GT (3:0, 3:1, 3:1.5) were electrospun to produce nanofiber. As shown in Fig. 1a & d, the electrospun pure PCL nanofibers had the average diameter of 156 ± 25 nm. PCL/GT (3:1) nanofibers showed spindle like beads (Fig. 1b & e). Other PCL/GT solution i.e., 3:1.5 combination resulted in beaded and irregular fiber geometries (Fig. 1c & f).

When PCL concentration was 15 %, four different compositions of PCL/GT (3:0, 3:1, 3:1.5, 3:3) were electrospun to get nanofibers. As shown in Fig. 2a & e, the electrospun pure PCL nanofibers had the average diameter of 288 ± 32 nm. PCL/GT (3:1) nanofibers showed an average diameter of about 187 ± 32 nm with very little bead density (Fig. 2b & f). However, when the ratio of PCL/GT reduced further to 3:1.5 and 3:3, nanofibers with more beads in the web were produced (Fig. 2c, g, d & h).

When the PCL concentration increased to 20%, a drastic difference in fiber morphology was observed. Five different compositions of PCL/GT (3:0, 3:1, 3:1.5, 3:3, and 3:6) were electrospun. In 3:0 compositions, microfibers with non-uniform morphology were obtained (Fig. 3a, f). For 3:1, and 3:1.5 PCL/GT compositions, fiber morphology was uniform with average fiber diameters of 389 ± 49% and 240 ± 53 nm, respectively (Fig. 3b, g, c & h). With changing the concentration to 3:3 and 3:6 blend ratio (PCL/GT), the morphology of the fibers changed to beaded structure (Fig. 3d, i, e & j). The addition of GT is found to decrease the diameter of PCL nanofibers. It was noticeable that, when the ratio of GT in the blend was equal or more than the ratio of PCL, electrospinning was difficult and the spinnability of the polymer solution was very poor. These results clearly revealed the effect of PCL concentration on the fiber diameter of the electrospun scaffold. At low PCL concentrations, because of the low viscosity of solution, defects in the form of beads and droplets were observed (Figs. 1 & 2). The process under these conditions showed both electrospraying and electrospinning. The results of the viscosity of PCL and PCL/GT (3:1.5) blends in different concentrations of PCL were shown in Table 1. When GT is blended with PCL, there is a significant decrease in viscosity of blends. Increasing the viscosity of blend solution from 300 to 1400 mPa/s by increasing polymer concentration resulted in smooth fibers with few beads and junctions [18]. From the above results, PCL/GT (3:1.5) with higher amount of natural biopolymer GT was selected as the optimum blend ratio for further experiments. The spinnability of different solutions that was assessed by performing surface tension analysis of GT, PCL, and PCL/GT was measured. GT solution subjected to electrospinning could not form nanofibers due to high surface tension (Table 2). However, when GT is blended with PCL, nanofibers were produced due to the lower surface tension of the solution [19].

3.2. Degradation behavior of nanofibers

Fig. 4 shows the morphological changes of electrospun scaffolds before and after in vitro degradation for 30 days period. Some breakage and change in morphology can be seen for nanofibers, but nanofibers keep their morphology after 30 days so they can be a good candidate as scaffolds.

3.3. FTIR results

FTIR analysis was carried out for surface characterization of PCL and PCL/GT nanofibers. Fig. 5 shows the FTIR spectra of PCL and PCL/GT (3:1.5) nanofibrous scaffolds. In PCL spectra, the peaks at 2942 and 1726 cm^{-1} represent the characteristic peaks for C–H and ester carbonyl groups, respectively. The major absorbance bands present in the spectra of GT were at 3442, 2930, 2856, 2158, 1747, 1635, 1441, 1367, 1243, 1080 and 1023 cm^{-1}. The broad band observed at 3442 cm^{-1} could be assigned to stretch vibrations of O–H groups in the gum tragacanth. The bands at 2930 and 2856 cm^{-1} correspond to stretching vibrations of methylene groups and the broad band at 2158 cm^{-1} shows various carbonyl species of the gum. The sharp peak at 1747 cm^{-1} could be assigned to carbonyl stretching vibrations in aldehydes, ketones and

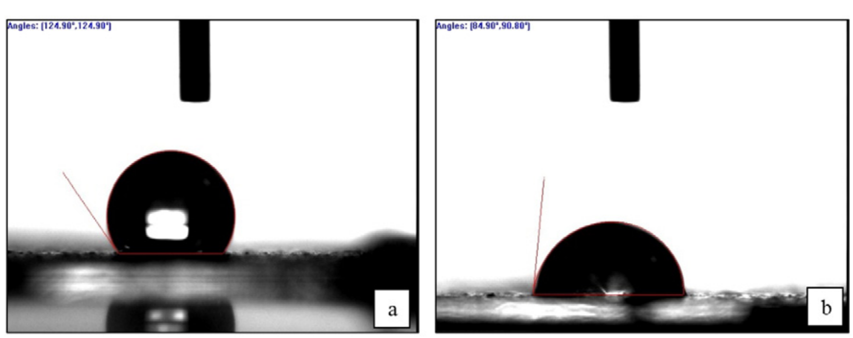

Fig. 9. Contact angle of electrospun nanofibers; a) PCL nanofibers, b) PCL/GT nanofibers.

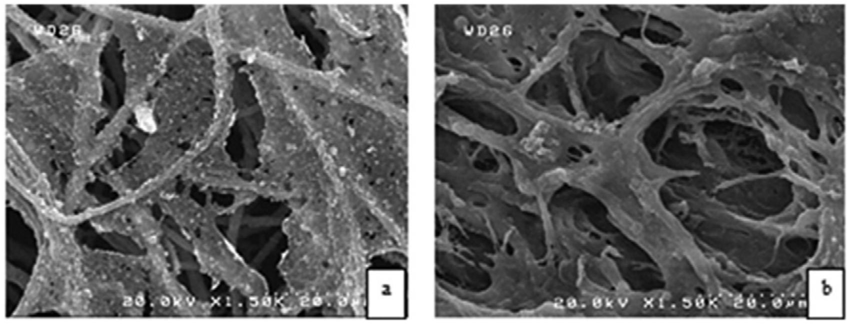

Fig. 10. Scanning electron micrographs of human fibroblast cell lines AGO cultured on electrospun PCL (10 w/v %), PCL/GT (3:1.5) nanofibers after 2 days of culture.

carboxylic acids. The stronger band found at 1635 cm^{-1} could be assigned to the characteristic of asymmetrical stretch of carboxylate group. Bands at 1441 and 1367 cm^{-1} could be attributed to symmetrical stretch of carboxylate groups and bands at 1441 and 1367 cm^{-1} showed the symmetrical stretch of carboxylate group. In PCL/GT scaffold, the O–H stretching has shifted to the lower frequency side and a sharp peak at 3433 cm^{-1} was observed. A slight bending at 1727 cm^{-1} is due to the presence of carbonyl group in PCL and another peak at 1166 cm^{-1} is due to C–O–C group.

3.4. DSC results

Fig. 6 shows the results of differential scanning calorimetric analysis of electrospun matrices of PCL, GT, and their blend nanofibers. For pure PCL the endothermic peak related to the melting of the crystalline phase is observed in a temperature range between 30 and 70 °C, with a maximum at 59.5 °C. However its glass transition temperature is about −57 °C. The DSC trace of GT exhibited a very broad endothermic peak starting from 48 °C and ending at 202 °C with the peak temperature at 120 °C. This transition is associated with the loss of water that corresponds to the hydrophilic nature of functional groups of the GT polymer. The heating–cooling run of this sample confirms the above hypothesis. When the sample heated at the rate of 10 °C/min, first up to 160 °C and then cooled to 0 °C/min and heated again, this peak vanished (Fig. 7). The major thermal decomposition at 259 °C was observed for the GT. The PCL/GT nanofibers showed a single melting peak almost at 63 °C. Very slight increase in melting peaks was observed due to the blending of PCL with GT nanofibers. This may be attributed to the different types of nucleation and growth of crystallization of the constituents of blend nanofiber [20,21]. It should be noted that the samples were dried in oven at 70 °C for 10 min prior to DSC analysis (Fig. 8).

DSC data can provide information regarding the miscibility of polymer blend systems [22]. In a DSC graph for an immiscible blend of two polymers, each polymer phase represents its T_g while only one T_g at the temperature between two T_gs of each component is observed for a homogeneous miscible blend without a phase separation [23]. Fig. 6 shows that the T_g of GT and PCL appears at about −47 °C and −59 °C respectively, whereas, the T_g of the blend appears at about −54 °C without any additional peaks compared to the thermograms of GT and PCL. With this one may conclude that the system is miscible.

3.5. Mechanical results

One of the most important properties of scaffolds for application in skin scaffolds is the mechanical property. Dressing must be able to withstand the load applied by cells [24] and may be strong enough to resist the forces of the body movement or outer environment. Artificial skin similar in structure to Integra has a tensile strength of 10 kPa, Young's modulus of 69 kPa, and maximum strain of 41% [25]. Whereas, hydrogel scaffolds can have tensile strengths in the order of 50–100 kPa, and maximum strain of 600–800%. Mechanical properties of nanofibrous wound dressings depend mainly on the material choice as well as its solution properties. The mechanical properties of the electrospun mats were shown in Fig. 9. The obvious decrease in tensile strength of PCL/GT scaffolds was mainly because of the blending of PCL with a natural polymer (GT) that has weak mechanical properties. The production of composite PCL/GT scaffolds provided a scaffold with tensile strength and maximum strain of 0.4 MP and 28.3% respectively.

3.6. Porosity of scaffolds

The porosity of electrospun nanofibers shows the space between the fibers, which is necessary for cell growth and cell adhesion. The porosity of PCL nanofibers electrospun from PCL in 90% acetic acid was about 85.7%. However in the blend nanofibers of PCL/GT, the porosity of webs increased to 88.4%. It could be due to the presence of non-uniformity in the web produced from the polymer blend solution.

3.7. Hydrophilicity of nanofibers

The hydrophilic/hydrophobic property of scaffolds can influence the initial cell adhesion and cell migration [26,27]. The contact angle of

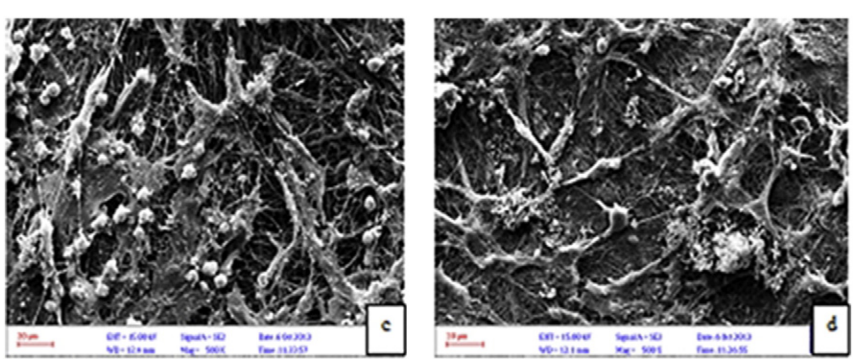

Fig. 11. Scanning electron micrographs of NIH 3T3 fibroblast cells cultured on a) electrospun PCL (10 w/v %), b) PCL/GT (3:1.5) nanofibers after 2 days of culture.

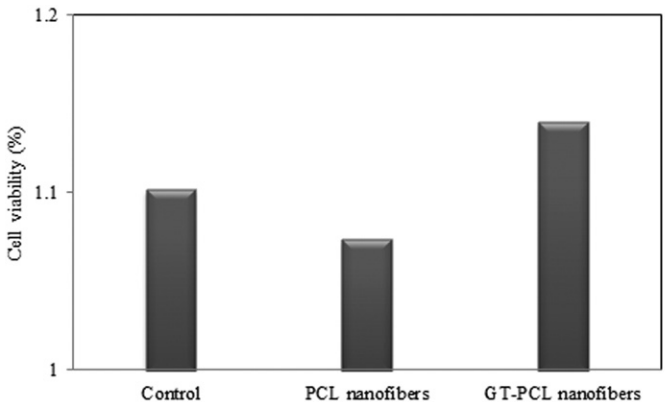

Fig. 12. MTT results of fibroblast cells on nanofibers in 3 days.

hydrophilic scaffolds is between 0° and 30° and less hydrophilic surfaces show a contact angle up to 90°. However, hydrophobic scaffolds show a contact angle more than 90°. From Fig. 9, PCL nanofiber was highly hydrophobic and the contact angle obtained for it is about $124.9 \pm 2°$. PCL/GT web shows a contact angle of $84.9 \pm 3°$, which indicates the hydrophilic nature of the blend nanofibrous web. In PCL/GT nanofibers, the trapped air between the nanofibers and pores at the nanofiber surface is easily removed by the incoming water molecules because the water soluble component (GT) is probably leaching out.

3.8. SEM study of scaffolds with cells

The well-blended GT-PCL nanofibrous matrix that integrates the favorable and distinctive biological properties of GT and mechanical properties of PCL is expected to significantly improve the material properties, while providing a stable, nurturing environment for a broad array of biomedical applications. Figs. 10 and 11 show the SEM micrographs of human fibroblast cell lines AGO and NIH 3 T3 fibroblast cells morphology and interaction between cells and nanofibrous webs after 48 h. Fibroblast cells on the scaffold containing GT stretched properly on the nanofibers and showed better proliferation. Our results exhibited that produced nanofibers from GT and PCL have the promising potential of being used as skin scaffolds.

3.9. Cytotoxicity evaluation

The results of MTT test in direct method are summarized in Fig. 12. The results showed that in PCL/GT nanofibers, proliferation is more than PCL nanofibers because the incorporation of GT created some hydrophilic groups on the surface of PCL/GT scaffolds, thus making them more favorable for cell growth and proliferation.

The toxicity of nanofibers from PCL/GT and PCL was studied by indirect cytotoxicity evaluation too. The cytotoxicity of various concentrations of the extract medium from the different nanofibers is shown in Fig. 13. When the 3T3 cells were incubated with various concentrations of the extraction media of nanofibers, there was an increase in average cell viability compared with control extract. However, the cell viability was increased when the concentration of the extract increased. So these nanofibrous mats are clearly proven to be safe.

3.10. Antibacterial properties

Antibacterial activity of PCL/GT and PCL nanofibers was investigated using disk shape webs. The PCL/GT samples showed the antibacterial property against gram-negative bacteria (*P. aeruginosa*) and gram-positive bacteria (*S. aureus*) and the zone of inhibitory was visible somewhat in the plate (Fig. 14). It is assumed that the L-sugars found in tragacanth (L-arabinose and L-fucose) are responsible for the resistance to microbial attack, since most organism would be unable to metabolize these foreign sugars [9].

4. Conclusion

There is always a need for new engineered polymeric biomaterials with ideal properties and functional adaptation for tissue engineering. In this article, nano-structured biodegradable fibers from PCL and GT were prepared with interconnected fibrous networks. Compared to pure PCL, GT addition resulted in a large reduction of fiber diameter and changing fiber morphology. Produced scaffolds from 7% GT and 20% PCL had better morphology, and composition of 3:1.5 (PCL/GT) with a high amount of GT was selected for further experiments. Human fibroblast and NIH 3T3 fibroblast cells adhered and proliferated well on PCL/GT scaffolds. Hydrophilicity nature of nanofibers, degradation behavior, mechanical strength, good morphology of cells on PCL/GT nanofibers and cytotoxicity assessing methods showed that these scaffolds are safe and have the potential to be developed as skin scaffolds or wound dressing patches.

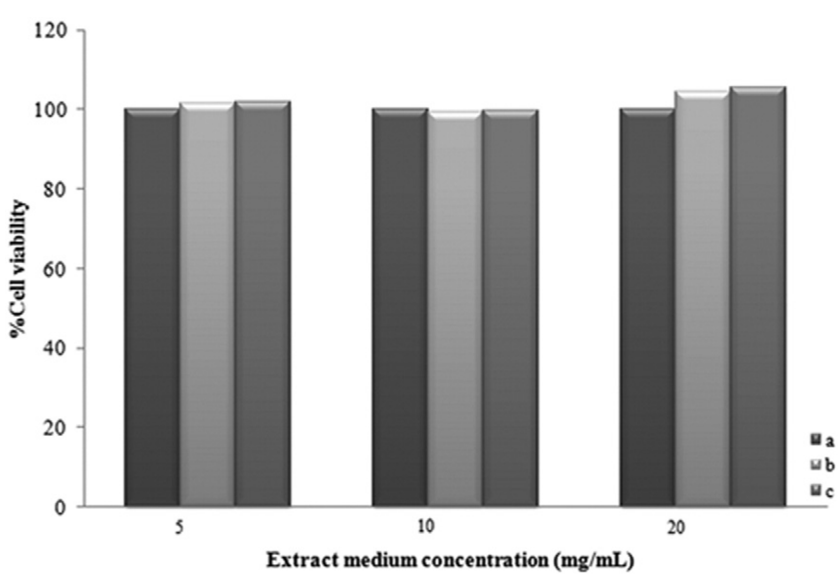

Fig. 13. Cytotoxicity tests from MTT assays of cell viability. a) control, b) PCL nanofiber, C) PCL/GT nanofiber.

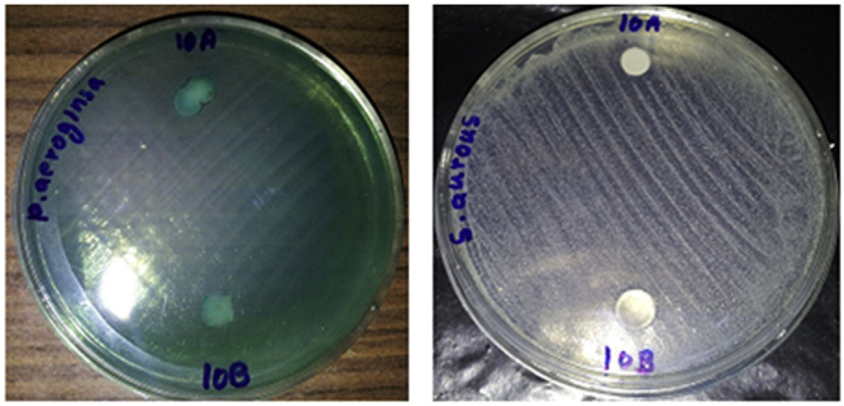

Fig. 14. Bactericidal activity of GT/PCL nanofibers with gram-positive *S. aureus* and gram-negative *P. aeruginosa*, A) PCL/GT nanofiber, B) PCL nanofiber.

Acknowledgment

Authors wish to thank the Center for Excellence Modern Textile Characterization, Tehran Iran for their support in providing the means for conducting experiments and Dr. M.A. Mohammadifar for his kind help. This study was supported by Iran National Science Foundation (INSF) under grant no. 91046806.

References

[1] T. Velnar, T. Bailey, V. Smrkolj, J. Int. Med. Res. 37 (2009) 1528–1542.
[2] D.L. Snyder, N. Sullivan, K.M. Schoelles, Skin Substitutes for Treating Chronic Wounds, Technology Assessment Report Project ID: HCPR0610 (Dec. 18, 2012).
[3] H. Yu, H. Xu, X. Chen, J. Hao, X. Jing, J. Appl. Polym. Sci. 101 (2006) 2453–2463.
[4] P. Zahedi, I. Rezaeian, S.O. Ranaei-Siadat, S.H. Jafari, P. Supaphol, Polym. Adv. Technol. 21 (2010) 77–95.
[5] J.P. Chen, G.Y. Chang, J.K. Chen, Colloids Surf. A Physicochem. Eng. Asp. 313 (2008) 183–188.
[6] B. Dhandayuthapani, U.M. Krishnan, S. Sethuraman, J. Biomed. Mater. Res. B Appl. Biomater. 94B (2010) 264–272.
[7] O. Suwantong, U. Ruktanonchai, P. Supaphol, Polymer 49 (2008) 4239–4247.
[8] D. Gupta, J. Venugopal, M.P. Prabhakaran, V.R. Dev, S. Low, A.T. Choon, S. Ramakrishna, Acta Biomater. 5 (2009) 2560–5269.
[9] R.L. Davidson, Handbook of Water-Soluble Gums and Resins, chapter 11, McGraw-Hill, New York, 1980.
[10] D.M.W. Anderson, M.M.E. Bridgeman, Phytochemistry 24 (1985) 2301–2304.
[11] G.O. Asinall, (Ed.), the polysaccharides, Vol. 1, Academic press Inc., New York pp. 415–421.
[12] M. Ranjbar-Mohammadi, S.H. Bahrami, M.T. Joghataei, Mater. Sci. Eng. C 33 (2013) 4935–4943.
[13] A.K. Moghe, R. Hufenus, S.M. Hudson, B.S. Gupta, Polymer 50 (2009) 3311–3318.
[14] AOAC, Official Methods of Analysis, Association of Official Analytical Chemists, AOAC International, Arlington, VA, 1984.
[15] L. Ghasemi-Mobarakeh, M.P. Prabhakaran, M. Morshed, M.H. Nasr-Esfahani, S. Ramakrishna, Biomaterials 29 (2008) 4532–4539.
[16] M.V. Jose, V. Thomas, K.T. Johnson, D.R. Dean, N. Elijah, Acta Biomater. 5 (2009) 305–315.
[17] J.P. Chen, G.Y. Chang, J.K. Chen, Colloids Surf. A Physicochem. Eng. Asp. 313–314 (2008) 83–188 (409–421).
[18] J.M. Deitzel, J. Kleinmeyer, D. Harris, N.C.B. Tan, Polymer 42 (2001) 261–272.
[19] J. Doshi, D.H. Reneker, J. Electrost. 35 (1995) 151–160.
[20] K. Cho, F. Li, J. Choi, Polymer 40 (1999) 1719–1729.
[21] H. Frensch, B.J. Jungnickel, Colloid Polym. Sci. 267 (1989) 16–27.
[22] L. Wang, Z. Zhang, H. Chen, S. Zhang, C. Xiong, J. Polym. Res. 17 (2009) 77–82.
[23] O. Olabisi, L.M. Robeson, M.T. Shaw, Polymer-Polymer Miscibility, Academic Press, New York, 1979, p. 117.
[24] M. Eastwood, R. Porter, U. Khan, G. McGrouther, R. Brown, J. Cell. Physiol. 166 (1996) 33–42.
[25] Y. Hong, A. Huber, K. Takanari, N.J. Amoroso, R. Hashizume, S.F. Badylak, W.R. Wagner, Biomaterials 32 (2011) 3387–3394.
[26] C.H. Kim, M.S. Khil, H.Y. Kim, H.U. Lee, K.Y. Jahng, J. Biomed. Mater. Res. 78 (2006) 283–290.
[27] H.S. Koh, C.K. Yong, C.K. Chan, S. Ramakrishna, Biomaterials 29 (2008) 3574–3582.